Energy & Environmental Science

Accepted Manuscript

ROYAL SOCIETY OF CHEMISTRY

www.rsc.org/ees

Graphical Abstract

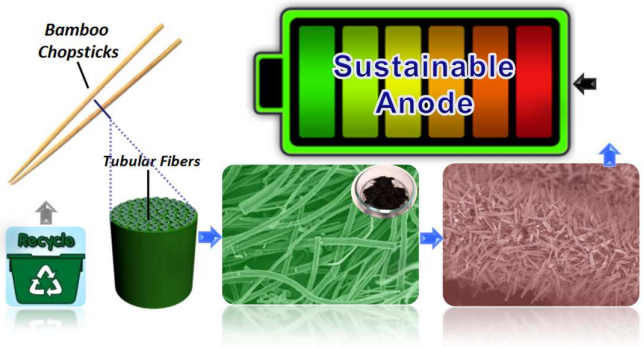

Uniform carbon fibers evolved from bamboo chopsticks garbage are achieved by a facile hydrothermal method, exhibiting competive electrochemical behaviors with commerical graphite, or pretty higher anodic performance after being optimized. Our work presents a smart and promising route to make sustainable anodes for LIBs industry, and economical state-of-art carbon-based hybrids available for other potential applications.

Broader context

Li-ion batteries (LIBs) nowadays play a dominant role on the progress of HEVs/EVs industry. However, despite the ceaseless development on electrode materials selection/manufacturing, current LIBs still show little promise to compete with the traditional gasoline in terms of price, energy, convenience and safety. Besides, the excepted huge exploitation on graphite driven by future demands will eventually lead to the depletion of natural graphitic resources one day. In a long-term perspective, LIBs therefore require to not only possess outstanding energy-storage capability but also be lower-cost and foremost sustainable. We herein propose a smart strategy to convert the used bamboo chopsticks into uniform carbon fibers for sustainable anode of LIBs. Abundant natural fibers in chopsticks waste are readily separated and dispersed after a simple hydrothermal treatment. The derived carbon fibers exhibit superior anodic performance compared to the bulky counterparts, and competive electrochemical behaviors and cost with commerical graphite. Moreover, their performance can be further upgraded by integrating nanostructured metal oxides onto each fiber. Our success in evolution of carbon fibers from chopsticks waste may provide a cost-effective and sustainable platform to develop advanced carbon-based materials for practical use, not merely in LIBs but also in other wide spectrum of fields.

Energy & Environmental Science

Cite this: DOI: 10.1039/c0xx00000x

ARTICLE TYPE

www.rsc.org/xxxxxx

Evolution of disposable bamboo chopsticks into uniform carbon fibers: A smart strategy to fabricate sustainable anodes for Li-ion batteries

Jian Jiang,[a] Jianhui Zhu,[a] Wei Ai,[a] Zhanxi Fan,[b] Xiaonan Shen,[a] Chenji Zou,[a] Jinping Liu,[d] Hua Zhang[b] and Ting Yu*[a,c]

Received (in XXX, XXX) Xth XXXXXXXXX 20XX, Accepted Xth XXXXXXXXX 20XX
DOI: 10.1039/b000000x

Future development of mini consumer electronics or large electric vehicles/power grids requires Li-ion batteries (LIBs) with not only the outstanding energy-storage performance but also a minimum cost, and the foremost sustainability. Herein, we put forward a smart strategy to convert used disposable bamboo chopsticks into uniform carbon fibers for anodes of LIBs. Bamboo chopsticks waste is recycled and simply treated by a controlable hydrothermal process performed in alkaline solutions, wherein abundant natural cellulose fibers in bamboo in situ get separated and dispersed spontaneously. After carbonizition, the evolved carbon fibers exhibit superior anodic performance to bulky bamboo carbons counterpart, and competive electrochemical behaviors and cost with commerical graphite. The performance of carbon fibers can be further upgraded by growing nanostructured metal oxides (like MnO_2) firmly on each fiber scaffold to form a synergetic core-shell electrode architecture. A high reversible capacity of ~710 mAh/g is maintained without decay up to 300 cycles. Our strategy presents a scalable route to transform chopsticks waste into carbon fibers, offering a very promising way to make sustainable anodes for LIBs and economical multi-functional carbon-based hybrids available for other practical applications.

1. Introduction

The ever-increasing market penetration of hybrid electric or all-electric vehicles (HEVs or EVs) requires not only the continual improvement of battery performance (particularly on fast charges output/storage) but also the minimization of battery cost as much as possible. Li-ion batteries (LIBs) based on the classic electrochemical system of carbonaceous anode and Li salts cathode (*e.g.*, layered $Li_{1-x}MO_2$, olivine $LiMPO_4$ and spinel $Li_{1-x}M_2O_4$, wherein M represents the transition metal) are superior to nickel-metal hydride batteries (Ni-MH) or ambient-temperature fuel cells in market.[1-3] They play a predominant role on the progress of HEVs/EVs industry owing to their attributes of high energy density, good rate performance, reliable stability and long lifespan.[2] Despite the ceaseless development of LIBs technology on electrode materials selection/manufacturing, the purchase cost of HEVs/EVs (mainly spent on LIBs units and related accessories) is yet far higher than that of mainstream gasoline-powered automobiles. Up to date, the current LIBs still show little promise of offering safe and sufficient capacity, with acceptable lifetime, good convenience and affordable price to compete with traditional fossil fuels.[4] In addition, the majority of commercially used anodic graphite stems from mineral deposits. Similar to the petroleum case in history, the prospective huge exploitation on graphite driven by future demands in EVs and large electricity grids would one day lead to the depletion of graphitic resources. The successful and large-scale commercial popularization of HEVs/EVs, in a longer-term perspective, is ought to rely on the advent of renewable, environmentally benign and cheaper electrode materials that are still with satisfactory electrochemical performance, preferably close to an infinite abundance in nature.[5]

The use of chopsticks brings about the mysterious verve of East Asia's catering culture but inevitably results in the negative environmental impacts and enormous waste of precious forest resources. Only in Japan, humans stupendously consume around a total of ~24 billion pairs of disposable chopsticks per year (adding up to millions of cubic meters of timber or fully grown bamboo trees).[6] This giant consumption gives rise to a great many of issues, in which the overriding concern is how to appropriately deal with the vast of discarded chopsticks garbage. Current handling approaches are still the conventional ones realized by either direct combustion of these wastes or sanitary landfills for biodegradation. Even though treatments in such ways are rather simple and convenient, they are virtually "low-level" and not rational, causing extra air/dust pollutions and more importantly making little use of these valuable and economic natural resources. How humans process the large amount of disposable chopsticks waste into commercially available products through

general, high-efficiency and cost-effective approaches is quite desirable but still needs reconsidering seriously.

We herein put forward a scalable and smart strategy to convert the disposable bamboo chopsticks waste into uniform carbon fibers for LIBs application. The recycled bamboo chopsticks only undergo a simple and controllable hydrothermal (delignification) treatment conducted in alkaline solutions, in which plenty of cellulose fibers in bamboo are in situ separated and dispersed spontaneously. Both the reaction time and alkali concentration are verified as significant parameters to adjust the overall fiber-separation process. Extracted natural fibers are further evolved into graphitic carbon fibers after a carbonization treatment. When tested as anode for LIBs, the chopsticks-derived carbon fibers can exhibit competitive anodic performance with practical graphitic materials, and much better electrochemical behaviors than unseparated bamboo carbons in terms of specific energy and rate capability. We also find the anodic performance of carbon fibers can be markedly upgraded by integrating nanostructured metal oxides (e.g., MnO_2) onto each carbon fiber. Thanks to the three-dimensional (3D) functionalized core-shell constructions, the hybrid products of C/MnO_2 NWs/carbon fibers have been demonstrated as excellent anode materials for LIBs, with good cyclic performance (maintaining ~710 mAh/g without decay up to 300 cycles) and outstanding rate capability. To our knowledge, their comprehensive anodic performance is among the best reported to date for the hybrid systems of MnO_2@carbon matrix. Our success in evolution of carbon fibers from chopsticks waste may not only open up the possibility of manufacturing sustainable high-performance anode materials for LIBs, but also set up an economical platform to prepare advanced hierarchical carbon-based hybrid materials that might be available in a large spectrum of practical applications.

2. Experimental Section

2.1 Synthesis of carbon fibers: The disposable bamboo chopsticks were used as the raw materials and recycled from the canteens of Nanyang Technological University (NTU). The cleaned bamboo chopsticks were initially processed into bamboo shavings (length: ~1.4 cm; width: ~0.2 cm; thickness: ~0.06 cm;) by using a penknife. Within the underlying hydrothermal treatment, 1g of bamboo shavings were put into a Teflon-lined stainless steel autoclave wherein a 70 mL of homogeneous 3M KOH solution was contained. Then, the autoclave was sealed and placed still in an electric oven at the temperature of 150 ^oC for 6h. When cooled down to room temperature natually, the samples were fetched out, collected by vacuum filtration with common filter paper, washed by ultrasonication in 150 mL distilled water just for one time and dried at 60 ^oC in electric oven. Next, the cotton-like products were calcined at 800 ^oC under the protection of Ar flow (flow rate: 80 ppm) for 2h, allowing for the adequate carbonization of bamboo fibers into carbon fibers. Last, the evolved carbon fibers are washed by 0.1 M HCl to remove the residual KOH and dried at 60 ^oC for 12h.

2.2 Synthesis of C/MnO_2 NWs/carbon fibers: The hybrid of C/MnO_2@carbon fibers were prepared via a simple hydrothermal treatment by using carbon fibers as the raw materials. In details, a glass slide with 0.2 g of "cotton-like" carbon fibers fixed on was put into a 100 ml Teflon-lined stainless steel autoclave containing a 50 mL of 0.04 M $KMnO_4$ solution. The autoclave was then sealed and kept in the electric oven at 150±0.1°C for 6 h. Next, the hybrid samples were fetched from the glass slide and cleaned by ultrasonication treatment for few seconds to remove MnO_2 nanoparticle debris. After that, the formed intermediates were soaked into a 50 mL 10 mmol glucose solution and kept still at 60±0.1 °C for 12 h. Last, the samples were taken out, dried in air and calcined at 550 ^oC in Ar flow (80 sccm) for 1 h.

2.3 Material Characterization: The crystalline structure and the morphology of carbon fibers were characterized using a transmission electron microscope (High-resolution TEM/TEM, JEM 2100F) and a field-emission scanning electron microscope (FESEM, JEOL JSM-6700F). X-ray powder diffraction (XRD) pattern was recorded by a Bruker D8 Advance diffractometer with Cu K_α radiation (λ=0.15418 nm). The mass of electrode materials was precisely measured on a microbalance (A&D Company N92, Japan) with an accuracy of 0.01 mg. Nitrogen adsorption-desorption isotherms were measured at 77 K with a Micromeritics analyzer (Belsorp Mini). Thermogravimetric analysis (TGA) was performed on a SDT600 apparatus under a heating rate of ~10 K/min in air. X-Ray photoelectron spectroscopy (XPS) spectrum was measured on a Perkin-Elmer model PHI 5600 XPS system with a resolution of 0.3~0.5 eV from a monochromated aluminium anode X-ray source. The Raman spectrum was obtained by using a Witech CRM200 Raman system with 532 nm excitation laser. Microscopy observations were conducted by a universal research microscope (OLYMPUS, BX51).

2.4 Electrochemical Testing/Characterization: The working electrodes were fabricated by the convention slurry-coating method. For details, carbon fibers, poly(vinylidene fluoride) (PVDF) binder and acetylene black were mixed in a mass ratio of 80:10:10 and dispersed/homogenized in N-Methyl-2-pyrrolidone (NMP) to form slurries. The homogenous slurry was then pasted onto a Cu foil (thickness: 10~15 μm) and dried at 100 ^oC for 10h under vacuum. The mass loading of fiber products on each current collector was controlled to be 2.5~4.0 mg/cm^2. Electrochemical measurements were all performed by using CR-2032 coin-type cells within a potential range of 0.005-3 V. Cells were assembled in an Ar-filled glove box (MBraun, Unilab; H_2O<0.1 ppm, O_2<0.1 ppm) by using Li foil as the counter and reference electrode. 1 M $LiPF_6$ dissolved in a 1:1 (v/v) mixture of ethylene carbonate (EC) and diethyl carbonate (DEC) was used as the electrolyte. The electrochemical impedance spectroscopy and cyclic voltammetry measurements were performed on an electrochemical workstation (CHI 760D, CH Instruments Inc., Shanghai) and the galvanostatic charge/discharge tests were conducted using a specific battery tester (NEWARE, Shenzhen). Prior to battery testing, all cells were aged for 8h.

3. Results and Discussions

3.1 Characterizations of Bamboo Chopsticks

Bamboo usually acts as an all-purpose problem solver and suits for a wide range of applications by virtue of its unique fibrous structures.[7] Bamboo chopsticks made of bamboo culms can be anatomically understood as an aggregation of numerous oriented cellulose fibers embedded in an interwoven ligneous matrix (See the the schematic in Fig. 1A). The tubular cellulose fibers (Mass

ratio: ~60%) biologically function as nutrient/water transport corridors between the root and the leaves, whereas the part of lignin (Mass ratio: 10%~20%), a sort of 3D highly cross-linked polyphenolic polymer,[8] plays a role of binding these fibers together. Microscopy observations on bamboo chopsticks have been shown in Fig. 1B-D. The closer inspection toward their transverse section reveals that there distribute a large quantity of micro-sized fibers in bamboo, particularly around or near the vascular bundles. Scanning electron microscope (SEM) images (Fig. 1E-H) also show the appealing microstructures of these natural fibers, with a tubular diameter ranging from 5 to 10 μm. The fibrous structure seems preferable for energy storage applications like supercapacitors and LIBs because the tubular architecture itself can provide large inner surface areas and enrich the electrochemically active sites when compared to the solid counterpart.[9] Note that on tubular wall of bamboo fibers there exist plenty of nanosized holes or cavities. These natural nanostructures that originally offer passages for biomass exchange between neighboring fibers are also favorable for energy storage, capable of supplying extra accesses to inside of microtubes and thus shortening the distances for ionic diffusion. Nevertheless, unfortunate is that bamboo fibers always bundle tightly with each other even after high-temperature carbonization or high-energy ball-milling treatments.[7] Though using techniques of boiling, soaking or mechanical extraction is helpful for the isolation of bamboo fibers, the yielded fiber products are rather rough.[10] Their diameters are usually centered at ~200 μm, signifying that at least hundreds of microfibers are still bundled together. Such bulky carbonized host materials are difficult to be completely permeated by electrolyte. This is unbeneficial for the kinetic intercalation/deintercalation of Li^+. In an effort to tap the full potential of each fiber for LIBs, advanced techniques of fiber extraction/dispersion with good scalability are highly encouraged.

3.2 Carbon Fibers Evolved from Bamboo Chopsticks

We hereby develop a simple and effective way of evolving bamboo chopsticks into individual carbon fibers to address the fibers extraction/dispersion issue above and enable each single carbon fiber applicable for Li storage. Fig. 2A displays the schematic of the entire evolution procedures. Recycled bamboo chopsticks are firstly cleaned and made into shavings followed by a hydrothermal treatment performed in an alkaline solution for lignin removal. During the hydrothermal process, the lignin part between neighboring bamboo fibers is gradually dissolving into the hot KOH solution. The trace for lignin removal/dissolution was captured by SEM observations (See Fig. S1). We need to stress that the use of KOH would never be a critical issue for the scale up of our synthetic procedures since such treatments with alkali have yet been adopted in varieties of industrial productions, especially in paper and printing/dyeing industries. After lignin removal, the cotton-like cellulose fibers mixed with residual KOH are further calcined at 800 ^oC under the protection of Ar flow. Particularly noteworthy is that our produced carbon fibers still maintain good toughness (no visible changes appear even after a press of 10-pound weight; See Fig. S2), totally unlike other fragile fibers made from cotton, silk or cobweb.[11] SEM and TEM observations (Fig. 2B-E; Fig. S3A) illustrate the yielded fibrous products are uniformly dispersed, having a fluffy texture and a large aspect ratio of several hundreds or even thousands magnitude (the mean diameter of single fiber is observed no more than 6 μm while its maximum length even reaches few centimeters upward). This special "ultrahigh-aspect-ratio" property would potentially endow the anodic electrode with outstanding high-rate performance by transferring electrons directly along the long 1D electronic conducting cables rather than in disordered particle networks through numerous interparticle contacts.[12] Another structural highlight is that on carbon fiber surface there homogeneously distributed with mesoporous pores (10~20 nm in dimensions), which are quite accessible for the deep insertion of Li^+ into the whole fiber region. The generation of these mesopores results from the activation process by means of alkali (KOH) corrosion to carbon materials at a high temperature ($6KOH + C \rightarrow 2K + 3H_2 + 2K_2CO_3$).[13] Fig. 2F shows the diameter distribution for a representative set of derived fiber samples. The fiber diameters are mainly varied from 2.4 to 6.4 μm with the highest distribution between 3.6 and 4.8 μm. In optimized states, we find that the minimum thickness of carbon fibers is even down to ~600 nm (see Fig. S3B and C). All these values are lower than that of pristine fibers (~10 μm) in bamboo chopsticks, attributing to the volumetric contraction of cellulose fibers when bamboo chopsticks are successively subjected to the delignification and carbonization treatments. XRD pattern (Fig. 2G) and Raman spectrum (Fig. 2H) are also used to characterize the carbon fibers. The well-defined two diffraction peaks present in XRD pattern correspond to (002) and (100) facets of hexagonal carbon (JCPDS No. 41-1487), respectively. Both diffraction peaks looks broad since the graphite domain/crystalline size is extremely small though specimens have yet been annealed at a temperature as high as 800 ^oC.[5a] According to Scherrer equation, the mean domain thickness is calculated to be ~1.85 nm from the full width at half-maximum values of (002) peak. This suggests that the graphitic domain is composed of 5~6 carbon layers (i.e., 1.85/0.34=5.44), marching well with the result of HRTEM observation (Fig. S3D). Raman spectrum shows two fingerprint peaks, involving a disorder-induced D band (1341 cm^{-1}) and an in-plane vibrational G band (1592 cm^{-1}). The G band has a bit higher peak intensity than D band (I_D/I_G ratio is ~0.96), indicative of a higher degree of graphitization than commercially used carbon cloth, carbon fiber papers or even carbon nanotubes in previous literatures.[14] The X-Ray photoelectron spectroscopy (XPS) measurement on carbon fiber surface (Fig. S4) discloses that there remain other elements like F (9.5 %), O (6.5 %) and Cl (1.0 %). The as-formed functional groups (e.g., C-O, C=O, C-F, C-Cl, etc.) are quite useful since they may contribute part of capacities via lithiation/delithiation or pseudocapacitive reactions. The N_2 adsorption-desorption isotherm with a hysteresis loop (inset in Fig. 2I) show typical "type I" characteristics (according to IUPAC recommendations) which are usually led by microporous solids especially for the instances of carbon materials.[15] The specific surface area for evolved carbon fibers is measured around ~808.25 m^2/g. Also, we have calculated the micropore size of fiber specimens based on the density functional theory (DFT) (Fig. 2I). The carbon fibers contain ~47% microporosity below 2 nm, with small mesopores centered among a range of 2~10 nm. The existence of such surface defects and hydrophilic

function groups as above is much helpful for the nucleation formation of other functionalized active materials on carbon surface.[16] This potentially enables the immobilization of high-capacity materials with robust mechanical adhesion to carbon fibers scaffold, eventually forming advanced core-shell synergetic hybrid electrode systems for LIBs. Moreover, we have measured the electrical performance of a single carbon fiber (Fig.S5). Its electrical resistivity is evaluated around ~10^{-1} Ω·cm (very close to that of metals), which is quite favorable for LIBs performance especially for high-rate lithiation/delithiation.

Seeking to control the entire preparation of bamboo fibers, we thereby carry out systematic studies on relationships between KOH concentration (C_{KOH}) and other significant parameters like the hydrothermal reaction time and weight losses of chopsticks. Fig. 3A and B successively display their reaction time (*t*) and percent loss in weight (*Wt%*) as a function of C_{KOH} at a constant hydrothermal temperature of 150°. When C_{KOH} is as much as 1M, the *t* of 15±2h needs to be spent for the complete extraction of bamboo fibers. This treatment gives rise to a *Wt%* up to ~31.3%. Upon the increase of C_{KOH} from 1M to 6M, the *t* has to be 9± 1.5h (for 2M), 6±0.5h (for 3M), 5±0.3h (for 4M), 4.75±0.25h (for 5M) and 4.5±0.2h (for 6M), corresponding to the *Wt%* of ~28.3%, ~22.7%, ~23.3%, ~26.7%, ~33%, respectively. As reflected by the experimental data and their fitting analysis, the fiber-extraction procedure is proved highly associated with *t* and C_{KOH} parameters. Using a high molar-ratio alkali solution is able to shorten the *t* by the acceleration of delignification process but in turn inevitably causes the dissolution of partial cellulose fibers (~21% solubility percentage in concentrated alkaline) as well as the high *Wt%*.[17] Nevertheless, though prolonging the hydrothermal time indeed eliminates the use of concentrated KOH solution, the corresponding *Wt%* is not the lowest since a long hydrothermal period would also result in the partial weight loss of biomasses. Considering the manufacturing cost and production efficiency of bamboo fibers, we eventually choose 3M KOH as the hydrothermal solution, along with a moderate *t* (6h) and the lowest *Wt%* (~22.7%). Moreover, we also pay close attention to other influence factors, typically like reaction conditions, as compared and summarized in Table 1. Underneath the 5h soaking treatment in either alkaline/acid solutions or neutral water, we fail to attain any cellulose fibers; there are actually no changes on bamboo chopsticks after the soaking process except for the ones soaking in alkaline aqueous solutions (with a slight weight loss of ~3-6% caused by the dissolution of biomasses in bamboo). As for events under a hydrothermal condition, high-quality bamboo fibers (3~6 μm) are harvested merely in 3M alkalis, instead of in 3M acids or neutral water (See optical/SEM observations in Fig. S6). Even though rough fibers with a mean diameter of ~30 μm (marked by arrows in Fig. S6D) are also yielded after a hydrothermal process conducted in acids, the as-formed products are substantially carbonized and become rather rigid/fragile, simultaneously accompanied by remarkable morphological changes (*e.g.*, structural collapses in some regions) and huge weight losses up to ~63%. The resultant carbonization may be induced by the complicated intermolecular dehydration, hydrolysis and condensation/polymerization of organics (like oligosaccharides, hemicelluloses or other molecules in bamboo biomass) in neutral/acid atmospheres when the hydrothermal temperature is held at 150 °C.[18]

3.3 The Performance of Carbon Fibers in LIBs

LIBs performance of derived carbon fibers has been evaluated by using coin-type half cells, in which Li metal foils are used as the counter and reference electrode. Cyclic voltammetry (CV) is initially used to examine the charge storage behavior of carbon fibers at a scanning rate of 0.5 mV/s over a potential range of 0.005-3.00 V *vs. Li/Li*$^+$ (Fig. 4A). In the 1st CV scan, there is a cathodic peak present over a wide region attributing to complex phase transitions caused by Li intercalation into carbonaceous fibers. An evident reduction peak emerges at 0.435 V but disappears in subsequent cycles, which is related to irreversible electrochemical processes typically like the trap of Li^+ ions in lattices, the electrolyte decomposition and the formation of solid electrolyte interfase (SEI) layer covered on carbon surface.[19] Redox reactions of Li insertion/extraction in the following cycles become highly reversible. Li-intercalation reactions take place below ~0.5 V (the capacity contribution within ~0.5-0.85 V is ascribed to faradic capacitive reactions on carbon fiber surface) while the broad anodic peak related to Li-deintercalation process launches at ~0.28 V, consistent with the cases of carbon species derived from biomass in pioneering works.[2c, 5a, 12c] The CV curves for the 2nd, 3rd and even 50th cycle nearly overlap with each other, suggesting the highly reversible and electrochemically stable performance of carbon fibers electrode.

The galvanostatic charge/discharge tests have been conducted at ~0.37C (1C=372 mA/g) for 800 cycles (Fig. 4B) to estimate the long-term cyclic behavior of carbon fibers. For comparison, unseparated bulky bamboo carbons (See SEM observations in Fig. S7C and D) with an average size of ~100 μm are also tested. The electrode of carbon fibers exhibits initial discharge and charge capacities of ~500 mAh/g and ~283 mAh/g, respectively. By contrast, the bulk bamboo carbons show a bit higher initial discharge capacity (up to ~535 mAh/g) but a much lower reversible charge capacity of ~208 mAh/g. This implies that carbon fibers possess a better reversibility than their bulky counterpart, with an upper initial Coulombic efficiency of ~56.6%. The value is definitely higher than that of bamboo carbons (~38.8%), and even comparable to that of transitional metal oxides.[20] For carbon fibers, the evident decrease in irreversible capacity loss during the 1st cycle may be thanks to the individual fibrous geometric features; In kinetics, Li^+ may not tend to be trapped because carbon fibers, the active host materials have been perfectly isolated and dispersed for the ease of Li^+ intercalation/deintercalation. Both electrodes show a trivial capacity reduction among the prime 30 cycles and later a capacity rise in subsequent steps. The specific capacity of carbon fibers rises from the bottom capacity of ~256 mAh/g to ~355 mAh/g with a growing rate of ~0.25 mAh/g per cycle and then stabilizes at ~360 mAh/g, which is more than the practical capacity of commercial graphite (~300-330 mAh/g) and capacity values of other carbon materials.[2c, 3c, 5a, 21a] Note that similar activation results have been reported on carbon-/silicon-based materials.[21] We believe that this capacity-rise phenomenon may result from the two aspects as follow. Within prime tens of cycles, the capacity of carbon fibers begins to revive from the minimum value. The origin of this activation is mainly attributed to the

delayed infiltration of electrolyte into carbon fibers.[21c] Around 100 cycles later, the repeated Li insertion/deinsertion process would gradually disrupt carbon fibers preferably at the structural defects. Fibers breaking may lead to more open-up places and accordingly provide more active sites available for Li storage. Besides, Li ions can go through such open-up regions and further diffuse a few nanometers deep into carbon fibers, which may lead to a continual capacity rise until the entire carbon fiber has been fully utilized. Despite bulky bamboo carbons also have excellent cycling stability and undergo a similar capacity-increase process, the delivered capacity is maintained at the level of ~250 mAh/g (~110 mAh/g less than that of carbon fibers and far below the practical standard), and the ramped rate is only ~0.15 mAh/g per cycle. Galvanostatic charge/discharge tests at programmed C rates are further carried out to examine their rate capability (Fig. 4C). The electrode of carbon fibers is primarily subjected to continuous cycling under varied current densities, successively at 0.46 C (171 mA/g), 0.92 C (342 mA/g), 1.39 C (517 mA/g), 2.77 C (1030 mA/g), 5.54 C (2060 mA/g) and 12.34 C (4590 mA/g) followed by charge/discharge cycles with currents switching back to 0.46C. Corresponding records on the relationship between the reversible capacity and the current density have been summarized in Fig. 4D. The capacity of carbon fiber electrode can fully recover or even surpass its former values upon continuously switching the current rates, capable of delivering a maximum capacity up to 353 mAh/g (at 0.46 C), 319 mAh/g (at 0.92 C), 292 mAh/g (at 1.39 C), 254 mAh/g (at 2.77 C) and 211 mAh/g (at 5.54 C), respectively. All these values are higher than those of bamboo carbons. Note that when the current suddenly jumps to 12.34C (4590 mA/g; cells charged/discharged in less than 1 min), the electrode of carbon fibers still retains a capacity of ~137 mAh/g, which is definitely beyond the value of bamboo carbons (~59 mAh/g) and other hard carbon materials;[2c] more strikingly, this value is even a bit higher than that of highly conductive carbon nanotubes (CNTs) measured at 10C (3720 mA/g).[3c] Above results highlight both the excellent rate capability and capacity retention of derived carbon fibers, showing a great promise to function as an alternative anodic substitute for graphite in LIBs. Electrochemical impedance spectroscopy (EIS) recorded in the frequency range of 1×10^6~0.01 Hz under open-circuit conditions is shown in the inset of Fig. 4C. The data fitted from the semicircle in high frequency range reveal the electrode of carbon fibers has a low charge-transfer resistance (R_{ct}) of ~24 Ω (pretty lower than that of bulky bamboo carbons (~61 Ω)), evidencing the individual carbon fibers possess better electrolyte infiltration and charge-transport capability than bulk. In low frequency range, the comparison toward the fitting line slope illustrates carbon fibers electrode exhibits less Warburg impedance (Z_w), which represents a significant parameter associated with the diffusion of Li^+ ions along the inter-space of graphitic carbons.[22] The above impedance spectra suggest the electrode of carbon fibers undergoes a fast Faradaic process and has lower activation energy for Li^+ diffusion into graphitic lattices. Even after deep cycling, the R_{ct} of carbon fibers does not change a lot (Fig. S8). Apart from the electrochemical testing/analysis, we also compare the cost of anodic materials made from chopsticks-derived carbon fibers and the commercially used graphite (See Table S1). The unit prices given out are all referenced to the recent literature[5a] and the global trade website *Alibaba.com*. Assuming each coin-type cell contains ~100 mg active anode materials, the use of carbon fibers would bring about around $30~41 for manufacturing 10000 cells in lab. The total amount is lower than that of graphite ($39~54), implying the cost advantage of evolved carbon fibers for LIBs industry.

Though carbon fibers are proved superior to bulky bamboo carbons and competent in sustainability, battery performance and cost (raw materials are renewable and all recycled from wastes) with graphite (a type of limited fossil/mineral resource), their energy density is yet problematic to meet the ever-growing demands for modern energy-storage applications. Aimed to upgrade their energy density, we have tried various strategies to optimize carbon fibers, either by the growth of functionalized metal oxides on each fiber scaffold or doping active elements (like B, N, F and P etc.) on/into the fibrous carbon host.[23, 24] One model example is the promotion of anodic performance by constructing carbon-coated MnO_2 nanowires (NWs) on carbon fibers, forming a smart sandwich-like hybrid (denoted as C/MnO_2 NWs/carbon fibers). The choice of MnO_2 as incorporated electrode materials is mainly given by factors like manufacturing complexity, environment friendliness, the cost and natural abundance. Another notable reason is that unlike other transition metal oxides with conversion reactions occurring above ~1 V,[14a, 18c, 24] MnO_2 has a low lithiation plateau of ~0.5 V *vs. Li/Li*$^+$ (approaching the value of carbon species). This is definitely below the lowest unoccupied molecular orbital (LUMO) of liquid organic electrolyte but still keeps higher than Li-reduction potential, enabling the generation of stable protective passivation layers on anode surface to ensure the cyclic durability and simultaneously avoiding the yield of detrimental Li dendrites for safety.[4] XRD measurement has clearly identified the formation of C/MnO_2 NWs/carbon fibers hybrid after a series of post-treatments (See Fig. S9A). Fig. 5A-C show representative SEM images of C/MnO_2 NWs/carbon fibers hybrid products. The samples geometrically inherit the fibrous features and possess intriguing hierarchical structures consisting of a carbon fiber inner core and MnO_2 NWs outer shells. According to above XRD record and the HRTEM observation (Fig. S9B), the produced oxide is identified as α-type MnO_2 within a space group of I4/m. In addition to being immobilized as a robust shell (shell thickness: 3~5 μm) on each carbon fiber surface, a uniform carbon layer with few nanometers thickness is intimately coated on MnO_2 NWs, as confirmed by high-resolution TEM observation (Fig. S9C, see arrows) and Raman spectrum (inset in Fig. 5B; Raman peaks at 505, 572 and 630 cm^{-1} corresponds to distinct Mn-O stretching modes of MnO_2 while the ones located at 1342 and 1576 cm^{-1} are fingerprints for the thin carbon layer). As a consequence, nanostructured MnO_2 with a high theoretical capacity of ~1230 mAh/g has been perfectly encapsulated into a carbon matrix (by refferring to the thermogravimetric analysis (TGA) in Fig. S10B, the mass ratio of MnO_2 in C/MnO_2 NWs/carbon fibers is determined to be ~45.7%). Such designed electrode architecture is quite favorable for LIBs application, alleviating the problems led by self-aggregation and intrinsically low electronic conductivity of MnO_2, as well as the lithiation-induced stresses. As a proof-of-concept demonstration of such

hybrid products in LIBs, we have evaluated the hybrid of C/MnO_2 NWs/carbon fibers (CV and charge-discharge curves are successively present in Fig. S10C and D). Also, we compare the cyclic behaviors of MnO_2/carbon fibers (without carbon coating) and the pristine carbon fibers. Fig. 5D displays their cyclic performance at 0.2 A/g in a potential range of 0.005-3 V. C/MnO_2 NWs/carbon fibers hybrid electrode delivers initial discharge/charge capacities of 1105 mAh/g and 706 mAh/g, respectively. The capacity loss may be attributed to: i) irriversible intercalation of Li^+ into carbon fibers, ii) irriversible conversion of MnO_2 with Li^+, and iii) the formation of SEI film on electrode surfaces. The reversibe discharge capacity after 300 cycles is still kept at ~710 mAh/g (nearly two times that of pristine carbon fibers and far higher than that of MnO_2/carbon fibers electrode), showing 93.8% retention of the 2nd discharge capacity. Fig. 5E shows the programmed cyclic responses of the hybrid products at varied current densities. Along with the increase of current rates from 0.2 A/g to 6 A/g, the electrode of C/MnO_2 NWs/carbon fibers still exhibits stabilized cyclic behaviors, with maximum discharge capacities of 706, 578, 532, 478, 398 and 241 mAh/g at 0.2, 0.4, 0.8, 1.6, 3.2 and 6.4 A/g, respectively. Even when the current abruptly jumps back to 0.2 A/g, the electrode is even able to deliver a higher reversible capacity of ~715 mAh/g. These results exclusively confirm the enhanced energy-storage and rate capabilities of C/MnO_2 NWs/carbon fibers hybrids over the pristine carbon fibers and the single-phased MnO_2 anode.[26] The high capacity retention and outstanding rate behaviors are mainly ascribed to synergetic effects between MnO_2 and the carbon matrix. On the one hand, nanostructured MnO_2 with large surface to volume ratio ensures the delievery of a high specific capacity for the hybrid electrode of C/MnO_2 NWs/carbon fibers. On the other hand, the inner carbon fibers backbone functions as the robust scaffold and electric cables for electrons transfer, whereas the uniform carbon layers on the outer surface of MnO_2 NWs are responsible for positive mechanical protections.

4. Conclusions

In summary, a facile and scalable approach has been developed to transform the bamboo chopsticks waste into carbon fibers for LIBs application. The recycled bamboo chopsticks are merely subjected to a simple and controllable delignification process conducted in alkaline aqueous solutions. The natural cellulose fibers in bamboo are then able to be separated and dispersed automatically. It is confirmed that the reaction time and the alkali concentration are both key parameters to control the whole fibre extraction process. The obtained natural fibers are further evolved into graphitic carbon fibers after a carbonization treatment. When evaluated as anode of LIBs, the derived carbon fibre products show comparable anodic performance to practical graphitic materials, and far better electrochemical behaviors than unseparated bulky bamboo carbons in specific energy and high-rate capabilities. The electrode performance of carbon fibers can be optimized by growing nanostructured metal oxides (typically like MnO_2) robustly on carbon fiber surface, leading to the formation of an appealing 3D synergetic core-shell electrode architecture. The as-designed hybrid electrode of C/MnO_2 NWs/carbon fibers has been verified as excellent anode materials for LIBs, with good cycling performance (~710 mAh/g without decay lasting 300 cycles) and excellent rate performance. The enhanced electrochemical performance is ascribed to the combination of carbon fibers, the robust backbone and conducting cable, and C/MnO_2 NWs firmly anchored to carbon fibers surface, forming a unqiue core-shell electrode architecture with great synergetic effects. This work provides a facile and effective way to evolve bamboo chopsticks waste into useful carbon fibers, and more importantly supplies a sustainable and cost-effective platform to develop advanced carbon-based materials for practical use, not merely in LIBs but also in other fields like biosensors and wave absorption, etc.

Acknowledgements

This work is supported by the Singapore National Research Foundation under NRF-RF award No. NRF-RF2010-07, A*Star SERC PSF grant 1321202101 and MOE Tier 2 MOE2012-T2-2-049. H. Zhang thanks the support from MOE under AcRF Tier 2 (ARC 26/13, No. MOE2013-T2-1-034), AcRF Tier 1 (RG 61/12, RGT18/13, RG5/13), and Start-Up Grant (M4080865.070.706022) in Singapore. This Research is also conducted by NTU-HUJ-BGU Nanomaterials for Energy and Water Management Programme under the Campus for Research Excellence and Technological Enterprise (CREATE), that is supported by the National Research Foundation, Prime Minister's Office, Singapore. The authors thank Prof. Sum Tze Chien at Nanyang Technological University for XPS testing.

Notes and references

[a] *Division of Physics and Applied Physics, School of Physical and Mathematical Sciences, Nanyang Technological University, 637371, Singapore Fax: (65) 6795 7981; Tel: (65) 6316 2962; E-mail: YuTing@ntu.edu.sg*
[b] *School of Materials Science and Engineering, Nanyang Technological University, 639798, Singapore;*
[c] *Graphene Research Centre, National University of Singapore, 117546, Singapore.*
[d] *Institute of Nanoscience and Nanotechnology, Department of Physics, Central China Normal University, Wuhan, 430079, Hubei, P.R. China.*

† Electronic Supplementary Information (ESI) available: SEM images of intermediate products during the fiber-extraction process; TEM image of a single carbon fiber; optical and SEM images of samples treated in different atmospheres; XRD pattern and TEM image of C/MnO_2 NWs/carbon fibers. See DOI: 10.1039/b000000x/

‡ *Jiang Jian* and *Zhu Jianhui* contributed equally to this work.

1 (*a*) P. G. Bruce, B. Scrosati and J.-M. Tarascon, *Angew. Chem. Int. Ed.*, 2008, **47**, 2930; (*b*) J.-M. Tarascon and M. Armand, *Nature*, 2001, **414**, 359.
2 (*a*) B. Kang and G. Ceder, *Nature*, 2009, **458**, 190; (*b*) B. L. Ellis, K. T. Lee and L. F. Nazar, *Chem. Mater.*, 2010, **22**, 691; (*c*) V. G. Pol and M. M. Thackeray, *Energy Environ. Sci.*, 2011, **4**, 1904.
3 (*a*) H. Li, Z. Wang, L. Chen and X. Huang, *Adv. Mater.*, 2009, **21**, 4593; (*b*) Y. Zhu, S. Murali, W. Cai, X. Li, J. Suk, J. R. Potts and R. S. Ruoff, *Adv. Mater.*, 2010, **23**, 3906; (*c*) H. Zhang, G. Cao and Y. Yang, *Energy Environ. Sci.*, 2009, **2**, 932; (*d*) L. Li, A. O. Raji and J. M. Tour, *Adv. Mater.*, 2013, **25**, 6298.
4 J. B. Goodenough, *Energy Environ. Sci.*, 2014, **7**, 14.
5 (*a*) W. E. Tenhaeff, O. Rios, K. More and M. A. McGuire, *Adv. Funct. Mater.*, 2014, **24**, 86; (*b*) J. Ding, H. Wang, Z. Li, A. Kohandehghan, K. Cui, Z. Xu, B. Zahiri, X. Tan, E. M. Lotfabad, B. C. Olsen and D. Mitlin, *ACS Nano*, 2013, **7**, 11004; (*c*) D. S. Jung, M.-H. Ryou, Y. J. Sung, S. B. Park and J. W. Choi, *PNAS*, 2013, **DOI: 10.1073/pnas.1305025110**.

6 (*a*) H. Dayle and L. Rachel, *Food and Nutrition*, New York: Marshall Cavendish Reference, USA, 2009, 1043; (*b*) Asia Times Online, Rising Chinese chopstick prices help Japan firm, http://www.atimes.com/atimes/China_Business/HD20Cb01.html. Accessed: September, **2011**.

7 (*a*) H. P. Khalil, I. Bhat, M. Jawaid, A. Zaidon, D. Hermawan and Y. S. Hadi, *Mater. Design,* 2012, **42**, 353; (*b*) S. Jain, R. Kumar and U. Jindal, *J. Mater. Sci.,* 1992, **27**, 4598; (*c*) L. Osorio, E. Trujillo, A. Van Vuure and I. Verpoest, *J. Reinf. Plast. Compos*., 2011, **30**, 396.

8 (*a*) R. K. Sharma, J. B. Wooten, V. L. Baliga, X. Lin, W. G. Chan and M. R. Hajaligo, *Fuel*, 2004, **83**, 1469; (*b*) H. Nimz, *Angew. Chem. Int. Ed.,* 1974, **13**, 313.

9 J. Jiang, Y. Li, J. Liu, X. Huang, C. Yuan and X. W. Lou, *Adv. Mater.,* 2012, **24**, 5166.

10 (*a*) M. Das and D. Chakraborty, *J. Appl. Polym. Sci.,* 2008, **107**, 522; (*b*) A. P. Deshpande, M. Bhaskarrao and C. L. Rao, *J. Appl. Polym. Sci.,* 2000, **76**, 83.

11 (*a*) F. Omenetto, D. Kaplan, *Science,* 2010, **329**, 528; (*b*) F. Vollrath, D. Porter, *Soft Matter,* 2006, **2**, 377.

12 (*a*) S. Ding, J. Chen and X. W. Lou, *Adv. Funct. Mater.,* 2011, **21**, 4120; (*b*) J. Jiang, Y. Li, J. Liu and X. Huang, *Nanoscale,* 2011, **3**, 45; (*c*) J. Chen, J. Z. Wang, A. I. Minett, Y. Liu, C. Lynam, H. Liu and G. G. Wallace, *Energy Environ. Sci.,* 2009, **2**, 393.

13 (*a*) Y. Zhu, S. Murali, M. Stoller, K. Ganesh, W. Cai, P. Ferreira, A. Pirkle, R. Wallace, K. A. Cychosz, M. Thommes, D. Su, E. A. Stach and R. S. Ruoff, *Science,* 2011, **332**, 1537; (*b*) Y. J. Kim, B. J. Lee, H. Suezaki, T. Chino, Y. Abe, T. Yanagiura, K. C. Park and M. Endo, *Carbon,* 2006, **44**, 1592.

14 (*a*) Y. S. Luo, J. S. Luo, J. Jang, W. W. Zhou, H. P. Yang, X. Y. Qi, H. Zhang, H. J. Fan, D. Y. Yu, C. M. Li, T. Yu, *Energy Environ. Sci.,* 2012, **5**, 6559; (*b*) J. Jiang, J. Liu, W. W. Zhou, J. H. Zhu, X. T. Huang, X. Y. Qi, H. Zhang and T. Yu, *Energy Environ. Sci.,* 2011, **4**, 5000; (*c*) Y. Luo, J. Jiang, W. Zhou, H. Yang, J. Luo, X. Qi, H. Zhang, D. Yu, C. M. Li and T. Yu, *J. Mater. Chem.,* 2012, **22**, 8634.

15 K. Sing, D. Everett, R. Haul, L. Moscou, R. Pierotti, J. Rouquérol and T. Siemieniewska, *Pure & Appl. Chem.,* 1985, **57**, 603.

16 (*a*) J. J. Xu, K. Wang, S. Z. Zu, B. H. Han and Z. X. Wei, *ACS Nano,* 2010, **4**, 5019; (*b*) J. Jiang, J. Liu, R. M. Ding, J. H. Zhu, Y. Y. Li, A. Z. Hu, X. Li and X. T. Huang, *ACS Appl. Mater. Interfaces*, 2011, **3**, 99.

17 J. Cai, L. Zhang, *Macromol. Biosci.,* 2005, **5**, 539.

18 (*a*) H. Wang, Z. Xu, A. Kohandehghan, Z. Li, K. Cui, X. Tan, T. Stephenson, C. K. King'ondu, C. M. B. Holt, B. C. Olsen, J. Tak, D. Harfield, A. O. Anyia and D. Mitlin, *ACS Nano,* 2013, **7**, 5131; (*b*) X. Sun, Y. Li, *Angew. Chem. Int. Ed.,* 2004, **43**, 597.

19 (*a*) B. Wang, J. S. Chen, H. B. Wu, Z. Y. Wang and X. W. Lou, *J. Am. Chem. Soc.,* 2011, **133**, 17146; (*b*) X. W. Lou, D. Deng, J. Y. Lee and L. A. Archer, *Chem. Mater.* 2008, **20**, 6562; (*c*) J. Jiang, J. Luo, J. Zhu, X. Huang, J. Liu and T.Yu, *Nanoscale,* 2013, **5**, 8105.

20 (*a*) J. P. Liu, Y. Y. Li, X. T. Huang, G. Y. Li and Z. K. Li, *Adv. Funct. Mater.,* 2008, **18**, 1448; (*b*) J. Liu, Y. Li, R. Ding, J. Jiang, Y. Hu, X. Ji, Q. Chi, Z. Zhu and X. T. Huang, *J. Phys. Chem. C,* 2009, **113**, 5336; (*c*) W. W. Zhou, C. W. Cheng, J. Liu, Y. Y. Tay, J. Jiang, X. T. Jia, J. X. Zhang, H. Gong, H. H. Hng, T. Yu and H. J. Fan, *Adv. Funct. Mater*., 2011, **21**, 2439.

21 (*a*) C. Masarapu, V. Subramanian, H. Zhu and B. Wei, *Adv. Funct. Mater.,* 2009, **19**, 1008. (*b*) H. L. Wang, Z. W. Xu, Z. Li, K. Cui, J. Ding, A. Kohandehghan, X. H. Tan, B. Zahiri, B. C. Olsen, C. M. B. Holt and D. Mitlin, *Nano Lett.*, 2014, **14**, 1987. (*c*) H. Wu, G. Yu, L. Pan, N. Liu, M. T. McDowell, Z. Bao, Y. Cui, *Nat. Commun.*, 2013, **4**, 1943.

22 (*a*) T. Abe, H. Fukuda, Y. Iriyama and Z. Ogumi, *J. Electrochem. Soc.,* 2004, **151**, A1120; (*b*) Y. C. Chang, J. H. Jong, G. T. K. Fey, *J. Electrochem. Soc.,* 2000, **147**, 2033.

23 (*a*) J. Luo, J. Liu, Z. Zeng, C. F. Ng, L. Ma, H. Zhang, J. Lin, Z. Shen, H. J. Fan, *Nano Lett.,* 2013, **13**, 6136; (*b*) B. Liu, J. Zhang, X. Wang, G. Chen, D. Chen, C. Zhou, G. Z. Shen, *Nano Lett.,* 2012, **12**, 3005; (*c*) W. Li, X. Wang, B. Liu, S. Luo, Z. Liu, X. Hou, Q. Xiang, D. Chen and G. Z. Shen, *Chem.-Eur. J.,* 2013, **19**, 8650; (*d*) Q. Xiong, J. P. Tu, X. Xia, X. Zhao, C. Gu and X. L. Wang, *Nanoscale,* 2013, **5**, 7906.

24 (*a*) Z. Wu, W. Ren, L. Xu, F. Li and H. Cheng, *ACS Nano,* 2011, **5**, 5463; (*b*) H. Wang, C. Zhang, Z. Liu, L. Wang, P. Han, H. Xu, K. Zhang, S. Dong, J. Yao and G. Cui, *J. Mater. Chem.,* 2011, **21**, 5430; (*c*) Z. Li, Z. Xu, X. Tan, H. Wang, C. M. B. Holt, T. Stephenson, B. C. Olsen and D. Mitlin, *Energy Environ. Sci.,* 2013, **6**, 871.

25 (*a*) N. Du, H. Zhang, B. Chen, J. Wu, X. Ma, Z. Liu, Y. Zhang, D. Yang, X. Huang and J. Tu, *Adv. Mater.,* 2007, **19**, 4505. (*b*) J. Lin, A. O. Raji, K. Nan, Z. Peng, Z. Yan, E. L. G. Samuel, D. Natelson and J. M. Tour, *Adv. Funct. Mater.,* 2014, **24,** 2044; (*c*) W. Zhou, Y. Tay, X. Jia, D. Wai, J. Jiang, H. Hoon, T. Yu, *Nanoscale,* 2012, **4**, 4459; (*d*) J. Jiang, J. Zhu, R. Ding, Y. Li, F. Wu, J. Liu and X. Huang, *J. Mater. Chem.,* 2011, **21**, 15969.

26 (*a*) A. Reddy, M. M. Shaijumon, S. R. Gowda and P. M. Ajayan, *Nano Lett.,* 2009, **9**, 1002; (*b*) H. Xia, M. Lai and L. Lu, *J. Mater. Chem.,* 2010, **20**, 6896; (*c*) J. Jiang, J. Zhu, Y. Feng, J. Liu, X. Huang, *Chem. Commun.,* 2012, **48**, 7471; (*d*) X. Li, D. Li, L. Qiao, X. Wang, X. Sun, P. Wang and D. He, *J. Mater. Chem.,* 2012, **22**, 9189.